LEGIBILITY NOTICE

A major purpose of the Technical Information Center is to provide the broadest dissemination possible of information contained in DOE's Research and Development Reports to business, industry, the academic community, and federal, state and local governments.

Although a small portion of this report is not reproducible, it is being made available to expedite the availability of information on the research discussed herein.

1

130/ 12/18/87 UB (2) DR 0347-6

ORNL/FEDC-87/2

POLOIDAL MAGNETICS OF A DIVERTOR COMPACT IGNITION TOKAMAK

D. J. Strickler
Y-K. M. Peng
S. C. Jardin

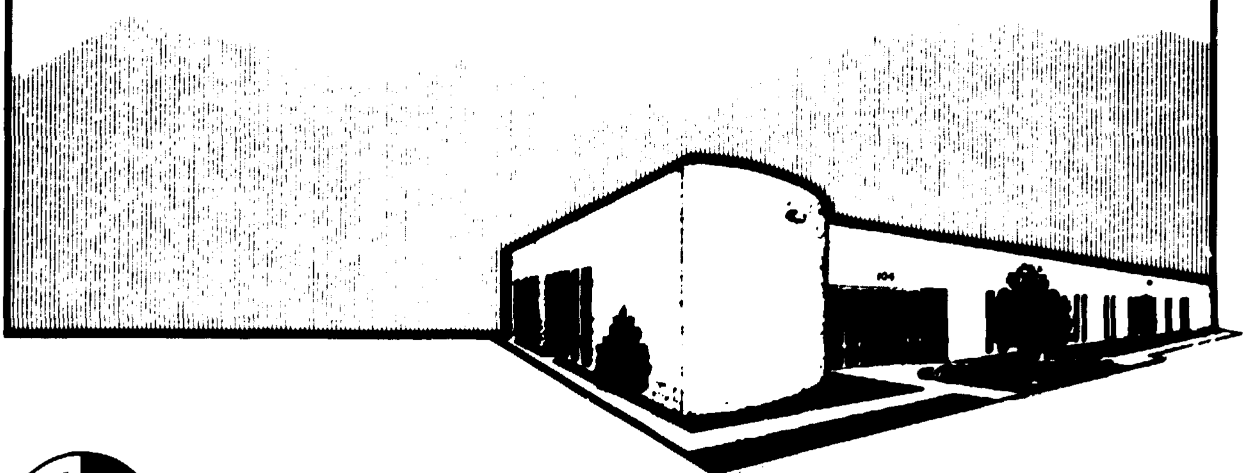

FUSION ENGINEERING DESIGN CENTER
OAK RIDGE NATIONAL LABORATORY
Operated by MARTIN MARIETTA ENERGY SYSTEMS, INC

Printed in the United States of America. Available from
National Technical Information Service
U.S. Department of Commerce
5285 Port Royal Road, Springfield, Virginia 22161
NTIS price codes—Printed Copy: A03; Microfiche A01

ORNL/FEDC--87/2

DE88 003648

ORNL/FEDC-87/2
Dist. Category UC-20 c,d

Fusion Energy Division

POLOIDAL MAGNETICS OF A DIVERTOR COMPACT IGNITION TOKAMAK

D. J. Strickler

Computing and Telecommunications Division
Martin Marietta Energy Systems, Inc.

Y-K. M. Peng

Fusion Engineering Design Center

S. C. Jardin

Princeton Plasma Physics Laboratory

Manuscript Completed — July 1987

Date Published — October 1987

Prepared by the
OAK RIDGE NATIONAL LABORATORY
Oak Ridge, Tennessee 37831
operated by
MARTIN MARIETTA ENERGY SYSTEMS, INC.
for the
U.S. DEPARTMENT OF ENERGY
under contract DE-AC05-84OR21400

CONTENTS

ABSTRACT

A technique is presented for calculating bounds on the poloidal field (PF) coil currents required to constrain critical plasma shape parameters when plasma pressure and current density profiles are changed. Such considerations are important in the conceptual design of the PF coils for the Compact Ignition Tokamak (CIT) and their electrical power systems in view of the uncertainty in plasma profiles and operating scenarios. Four relatively independent coil groups are sufficient to find a coil current distribution and equilibrium satisfying a prescribed plasma major radius, minor radius, and divertor strike point coordinates. The variation in the coil current distribution with plasma profiles tends to be large for external PF systems and provides a measure by which coil configurations may be compared.

1. INTRODUCTION

In the design of a divertor for an ignition tokamak,[1] it is assumed that the separatrix flux surface of the plasma meets the divertor plates at precise locations, referred to here as "strike points" (Fig. 1). The heat load on the divertor plates is sensitive to changes in the locations of these strike points. Further design constraints on the plasma shape include accurately positioning the outer edge of the plasma with respect to the radio-frequency (rf) wave launcher and limits on the plasma scrape-off relative to the inboard vacuum vessel.

These requirements lead to several design problems for poloidal field (PF) coil configurations. Among these are the feasibility of external PF coils [i.e., not linked with the toroidal field (TF) coils] in maintaining the plasma position and strike points and the dynamic control of these parameters using some combination of internal and external coils.

We consider the first of these problems in this study and show the sensitivity of the coil current distribution to changes in the plasma pressure and current density

ORNL-DWG 87-2083 FED

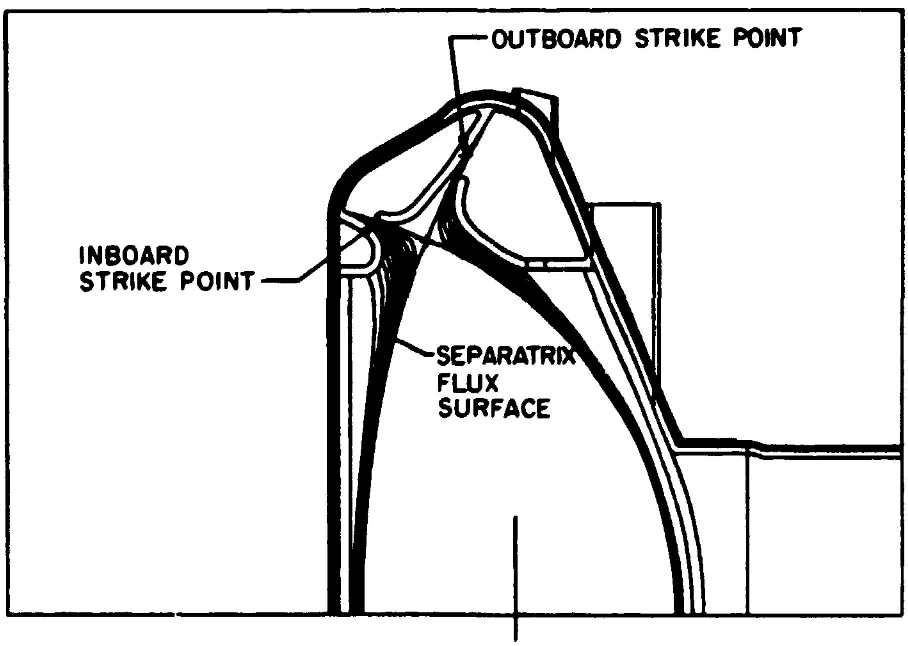

Fig. 1. CIT vacuum vessel and divertor configuration, showing the strike points where the separatrix flux surface meets the divertor plates.

profiles for a given PF coil system. The variation of the coil current distribution is used as a measure by which different PF coil configurations can be compared.

2. THE COMPACT IGNITION TOKAMAK POLOIDAL FIELD SYSTEM

The geometry considered here is based on a design of the Compact Ignition Tokamak (CIT)[2] with major radius $R_0 = 1.339$ m, minor radius $a = 0.411$ m, field on axis $B_t = 10.3$ T, and plasma current $I_p = 9.0$ MA. The external PF coil system is similar to that developed for the $R_0 = 1.2$ m CIT conceptual design[3] and consists of seven coil groups labeled PF1 through PF7 (Fig. 2) that provide the equilibrium vertical field, shaping field, and inductive flux for an elongated ($b/a = 2.3$) divertor plasma. Although the CIT PF system design includes windings internal to the TF coils, it is hoped that these can be reserved for dynamic control and carry minimal currents.

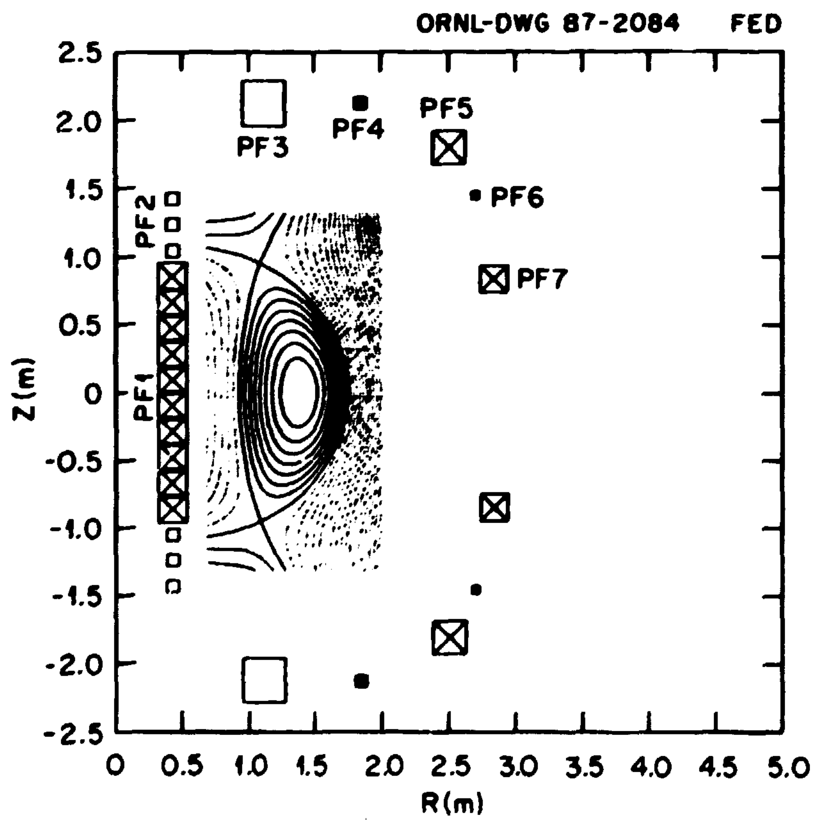

Fig. 2. Poloidal field coil configuration for a divertor CIT.

The central solenoid stack is split into two sections, PF1 and PF2, for added flexibility in providing a field null at startup and shaping the plasma cross section through a discharge. In this CIT design, the position and size of the shaping field coil PF3 are constrained by a structural press on the coil's inboard side and by access for a vertical diagnostic port through the plasma major radius on its outboard side. Coils PF4 and PF6 are in series with the lower element of the central solenoid, PF1. The outer ring coils, PF5 and PF7, provide the major components of the vertical field, but PF5 also makes a large contribution to the shaping field or higher-order derivatives of the external field. In general, all of the external PF coils contribute to the equilibrium, control, and shaping of the CIT plasma and to the flux change, which induces the plasma current and ohmically heats the plasma.

3. COMPUTING THE COIL CURRENT DISTRIBUTION

The first problem we consider is that of constraining a symmetric, divertor plasma boundary to pass through two points on the midplane, $(R_0 - a, 0)$ and $(R_0 + a, 0)$, and constraining the separatrix flux surface to intersect prescribed inner and outer strike points, (R_I, Z_I) and (R_O, Z_O), using external PF coils. The free-boundary tokamak magnetohydrodynamic (MHD) equilibrium code NEQ[4] is used in a mode in which the plasma is limited by a poloidal separatrix, and the current in one pair of coils, PF7, is adjusted to make the separatrix flux surface pass through $(R_0 + a, 0)$. The numerical software package HYBRD1[5] is used to determine the remaining free coil currents as roots of the equation

$$F(I_0) = 0 , \qquad (1)$$

where

$$F = \begin{bmatrix} (\psi_I - \psi_x)/\psi_x \\ (\psi_O - \psi_x)/\psi_x \\ (a - a_0)/a_0 \end{bmatrix} , \quad I_0 = \begin{bmatrix} I_{PF2} \\ I_{PF3} \\ I_{PF5} \end{bmatrix} ,$$

a_0 is a given plasma minor radius, and ψ_I, ψ_O, and ψ_x are the values of the poloidal magnetic flux at the inboard strike point, outboard strike point, and separatrix, respectively. For fixed currents in the coil groups PF1, PF4, and PF6 and given plasma profile functions, HYBRD1 calls NEQ as a subroutine to obtain values of the function F and solves for the coil currents I_θ. For a good initial guess of the solution vector, it typically takes seven to nine equilibrium calculations to converge to a solution (Fig. 3). The result is a set of CIT PF coil currents $I = (I_{PF1}, \ldots, I_{PF7})$ that satisfy the desired properties.

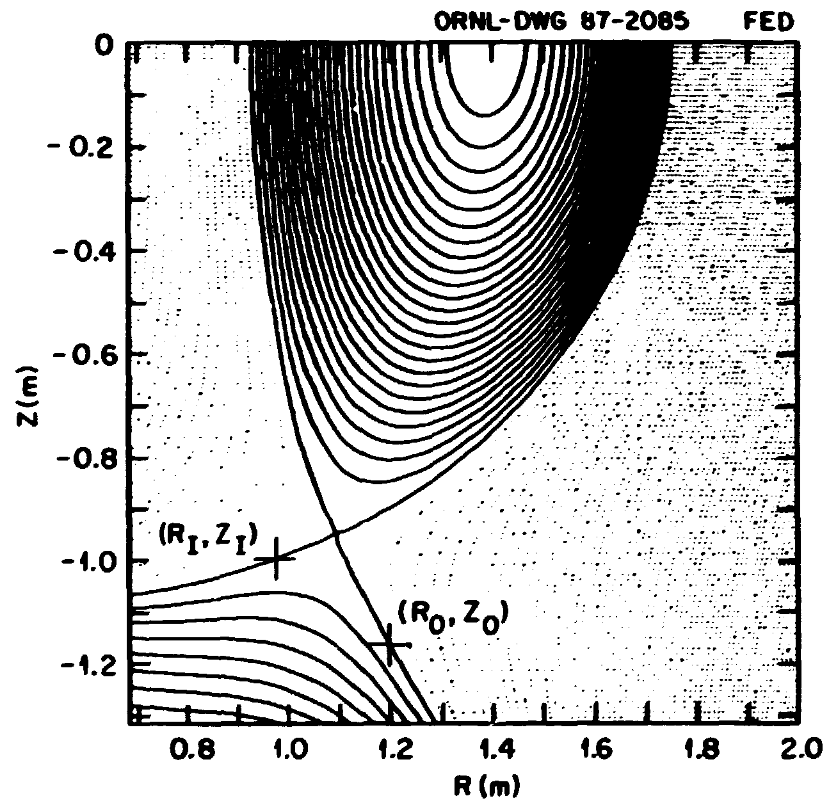

Fig. 3. Poloidal flux surfaces for a CIT divertor plasma with separatrix flux surface intersecting prescribed strike points, (R_I, Z_I) = (0.974 m, 0.996 m) and (R_O, Z_O) = (1.196 m, 1.162 m).

4. EFFECT OF PROFILE VARIATIONS

In the free-boundary solution of the MHD equilibrium equation

$$R^2 \nabla \cdot (R^{-2} \nabla_\psi) = -\mu R J(R, Z) \quad (2)$$

for the poloidal flux ψ, the plasma current density is given in terms of the plasma pressure, $P(\psi)$, and toroidal magnet flux function, $F(\psi) = RB_t$, as

$$J = R\, dP/d\psi + F/(\mu R)\, dF/d\psi\ . \tag{3}$$

In this analysis, we consider profile functions of the form

$$dP/dx = P_0(e^{-Ax} - e^{-A})/(e^{-A} - 1)\ , \tag{4a}$$

$$dF^2/dx = 2\mu R_0^2 P_0(1/\beta_J - 1)(e^{-Bx} - e^{-B})/(e^{-B} - 1)\ , \tag{4b}$$

where $x = (\psi - \psi_0)/(\psi_x - \psi_0)$; ψ_0 and ψ_x are values of the poloidal flux at the magnetic axis and separatrix, respectively. NEQ solves Eq. (2) with Dirichlet boundary conditions on a rectangular mesh (with dimensions of 65×129 for this study), scaling the parameter P_0 in Eq. (4) during the iterative procedure so that the total plasma current $I_p = \iint J\, dR\, dZ$ is fixed.

Plasma current profiles are characterized by the safety factor profile,

$$q = RB_t/(2\pi) \oint 1/(R^2 B_p) dl\ , \tag{5}$$

where the integral is along the contour of a poloidal flux surface. For divertor equilibria, where $B_p = 0$ at the separatrix, it is convenient to define a "mean-field" safety factor,

$$\bar{q} = RB_t/(2\pi \bar{B}_p) \oint 1/R^2 dl \tag{6}$$

(where $\bar{B}_p = \oint B_p dl / \oint dl$ is the average poloidal field on a flux surface), which is less sensitive to the presence of the poloidal separatrix, yet retains the dependence on toroidicity and plasma shape. At the plasma edge, the mean-field safety factor in this study takes on values of $\bar{q} = 2.6$–2.7, depending on the location of the poloidal separatrix.

For volume-averaged beta values near the Troyon limit[6] ($\beta_T = 0.03 I_p a B_t$), we use $\beta_J = 0.88$ in Eq. (4), resulting in $\langle\beta\rangle = 6.2$–$6.4\%$. We set $A = B$ and vary this profile parameter over the interval $-4.5 \le A \le -1.5$, obtaining a set of plasma current density distributions representing a range of uncertainty in J (Fig. 4), with associated mean-field safety factor values on axis of $0.8 \le \bar{q}_{axis} \le 1.1$ (Fig. 5). The solution vectors (Table 1) indicate a large redistribution of coil currents and a change in the direction of the current in PF5, which are undesirable for electrical systems design.

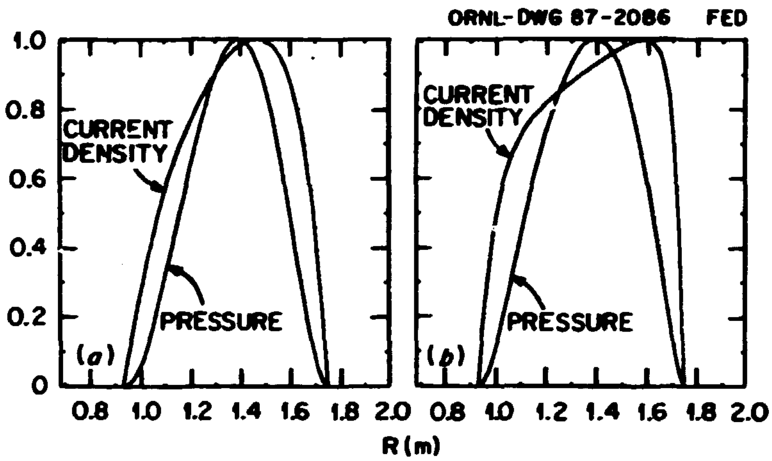

Fig. 4. Plasma pressure and current density profiles corresponding to profile parameters [Eq. (4)] $\beta_J = 0.88$ and (a) $A = B = -1.5$, (b) $A = B = -4.5$.

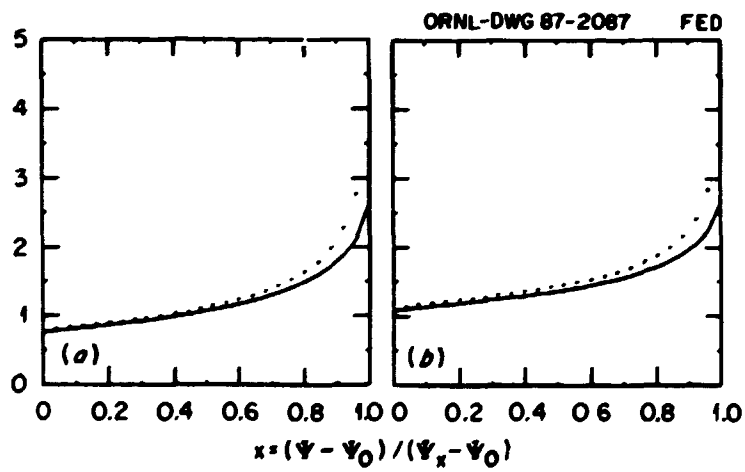

Fig. 5. Plasma mean field safety factor $\bar{q}$ (solid) and MHD safety factor q (dotted), corresponding to profile parameters [Eq. (4)] $\beta_J = 0.88$ and (a) $A = B = -1.5$, (b) $A = B = -4.5$.

Table 1. Value of $\bar{q}_{axis}$, location of divertor null point, and PF coil current distributions for a CIT divertor plasma with $R_0 = 1.339$ m, $a = 0.411$ m, inboard divertor plate strike point $(R_I,\ Z_I) = (0.974$ m, 0.996 m), and outboard divertor plate strike point $(R_O,\ Z_O) = (1.196$ m, 1.162 m), for $\beta_J = 0.88$ and $A = B$ in Eqs. (4a) and (4b). Fixed currents: $I_{PF1} = 15.0$ MA, $I_{PF4} = 0.488$ MA, $I_{PF6} = 0.225$ MA.

	Profile parameter A	
	−1.5	−4.5
$\bar{q}_{axis}$	0.8	1.1
Divertor null point		
R_x, m	1.104	1.089
Z_x, m	0.955	0.951
I_{PF2}, MA	−6.567	−3.465
I_{PF3}, MA	−3.780	−9.174
I_{PF5}, MA	−1.772	4.760
I_{PF7}, MA	−6.164	3.050

By changing the magnitude of the current in coil groups that are in series with the central ohmic heating (OH) solenoid element by $\Delta I_{PF1} = 1$ MA, $\Delta I_{PF4} = 0.032$ MA, and $\Delta I_{PF6} = 0.015$ MA and applying the same analysis, we find an "OH" coil current distribution $\Delta I^{(OH)} = (1.000, 0.776, 0.304, 0.032, -0.076, 0.015, 0.030)$. The flux linkage to the plasma, $\Delta\psi_{PF} = \sum M_{ip} I_i$, may be adjusted by adding a multiple of this OH distribution to a given solution vector without altering the plasma shape or strike point coordinates. For example, adding $\Delta I = 2.5\Delta I^{(OH)}$ to the solutions given in Table 1 (case 1 in Table 2) increases the PF flux swing by $\Delta\psi_{PF} = 1.9$ V·s (case 2 in Table 2). For given $\Delta\psi_{PF}$ and $\langle\beta\rangle$, bounds on the magnitude of currents in each coil group (with respect to a given range of profile uncertainty) are then completely determined by the OH distribution together with a set of solution vectors such as those given in Table 1.

It is insufficient, however, to compute the minimum and maximum coil currents for only the high-beta state. Bounds on PF coil current for use in electrical system design must be determined for all possible operating scenarios. For given currents

Table 2. Coil current distributions, divertor null location, and variation in poloidal field volt-seconds for a CIT divertor plasma with prescribed major and minor radii, prescribed divertor strike point coordinates, and two sets of fixed currents in coil groups PF1, PF4, and PF6

	Case 1	Case 2
Fixed coil currents, MA		
I_{PF1}	15.000	17.500
I_{PF4}	0.488	0.569
I_{PF6}	0.225	0.263
Coil current distributions, MA		
I_{PF2}	−6.567	−4.426
I_{PF3}	−3.780	−3.019
I_{PF5}	−1.772	−1.963
I_{PF7}	6.164	6.239
Divertor strike point		
R_x, m	1.104	1.106
Z_x, m	0.955	0.954
PF volt-seconds $\Delta\psi_{PF}$, V·s	16.31	18.24

in the coil groups in series with PF1 (i.e., PF4 and PF6), limits on coil current magnitudes may be set by the requirements for operating at less than the design value of beta. Table 3 lists coil currents associated with $\beta_J = 0.44$, for which average beta values are about half the Troyon limit. A comparison of Tables 1 and 3 indicates that, for comparable values of the mean-field safety factor on axis, the maximum current in coil PF2 required to fix the plasma shape and strike points occurs at low beta, while the remaining limiting current magnitudes are at high beta.

Table 3. Value of $\bar{q}_{axis}$, location of divertor null point, and PF coil current distributions for a CIT divertor plasma with prescribed major radius, minor radius, and divertor plate strike point coordinates, for $\beta_J = 0.44$ and $A = B$ in Eqs. (4a) and (4b). Fixed currents: $I_{PF1} = 15.0$ MA, $I_{PF4} = 0.488$ MA, $I_{PF6} = 0.225$ MA.

	Profile parameter A	
	−1.0	−3.0
$\bar{q}_{axis}$	0.8	1.1
Divertor null point		
R_x, m	1.110	1.094
Z_x, m	0.956	0.950
I_{PF2}, MA	−8.625	−5.928
I_{PF3}, MA	−3.816	−8.421
I_{PF5}, MA	−1.425	4.171
I_{PF7}, MA	5.563	2.883

5. COMPARISON OF COIL SYSTEMS

In order to compare the merits of two PF coil systems for a divertor plasma, it is useful to have a set of measures of the relative efficiency of a given coil arrangement in maintaining a plasma shape. For fixed plasma major radius, minor radius, and strike point coordinates, we measure the variation in the coil current distribution by the quantity

$$\Delta I = \left[\sum (I_i - I_i')^2 \Big/ \sum I_i^2\right]^{1/2} , \tag{7}$$

where $I = (I_1, \ldots, I_n)$, $I' = (I_1', \ldots, I_n')$ are the coil currents associated with plasma current density profiles J and J'. A measure of the change in the plasma shape (e.g., plasma elongation and triangularity) is given by

$$\Delta x = [(R_x - R_x')^2 + (Z_x - Z_x')^2]^{1/2} , \tag{8}$$

where (R_x, Z_x) and (R_x', Z_x') are the coordinates of the null points corresponding to current density profiles J and J'.

As an example, we use the first of these measures [Eq. (7)] to point out the advantage of internal PF windings. For I associated with $\bar{q}_{axis} = 0.8$, the solutions listed in Table 1 give a variation of $\Delta I = 0.508$. Introducing two pairs of internal windings (Fig. 6), labeled C1 and C2, we replace two elements of the solution vector I_0 [Eq. (1)], I_{PF3} and I_{PF5}, with I_{C1} and I_{C2} and then compute a new solution for the profile J' (defined by $\beta_J = 0.88$, $A = B = -1.5$). This set of solutions (Table 4) results in a variation $\Delta I = 0.039$, a significant reduction over the all-external coil system. Further, no coil currents change direction because of profile differences.

This example may be summarized by plotting the coil currents associated with the broad plasma current profile (J) vs those associated with the peaked profile (J'), as is done in Fig. 7; the variation in the coil current distribution is represented by the distance from the diagonal. It is clear that other strategies exist for using internal coils to minimize ΔI, some of which result in lower total coil currents.

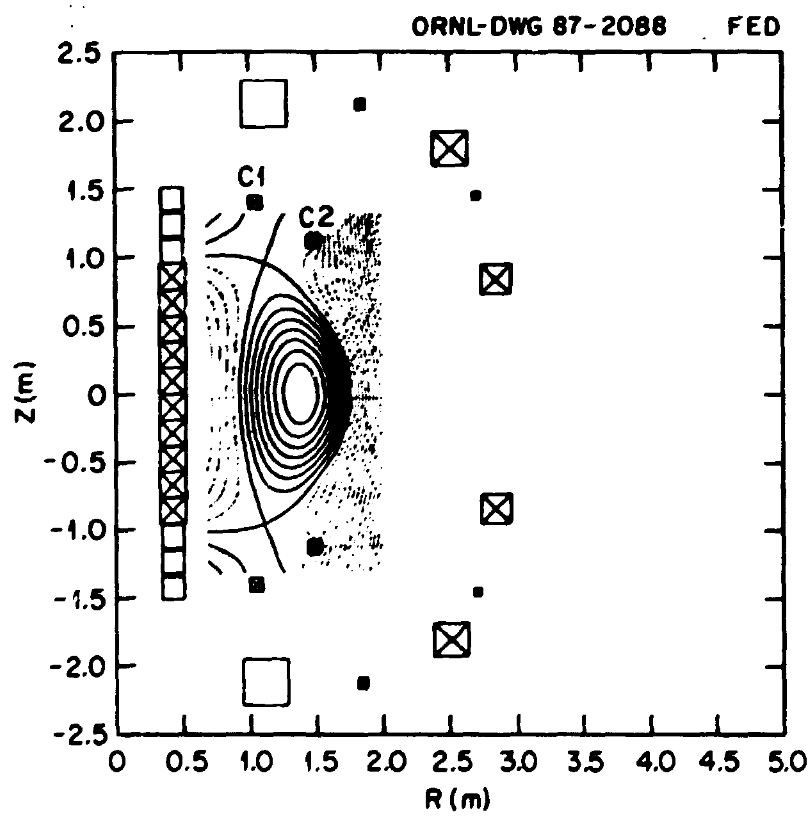

Fig. 6. Poloidal field coil system for a divertor CIT, including internal conductors C1 and C2.

Table 4. Value of $\bar{q}_{axis}$, location of divertor null point, and PF coil current distributions for a CIT divertor plasma with prescribed major radius, minor radius, and divertor plate strike point and with internal coils C1 and C2 used to produce a peaked plasma current profile. Fixed currents: $I_{PF1} = 15.0$ MA, $I_{PF3} = -9.174$ MA, $I_{PF4} = 0.488$ MA, $I_{PF5} = 4.760$ MA, $I_{PF6} = 0.225$ MA.

	Profile parameter A	
	−1.5	−4.5
$\bar{q}_{axis}$	0.7	1.1
Divertor null point		
R_x, m	1.117	1.089
Z_x, m	0.956	0.951
I_{PF2}, MA	- 6.993	−3.465
I_{C1}, MA	0.755	0.000
I_{C2}, MA	−0 779	0.000
I_{PF7}, MA	3.597	3.050

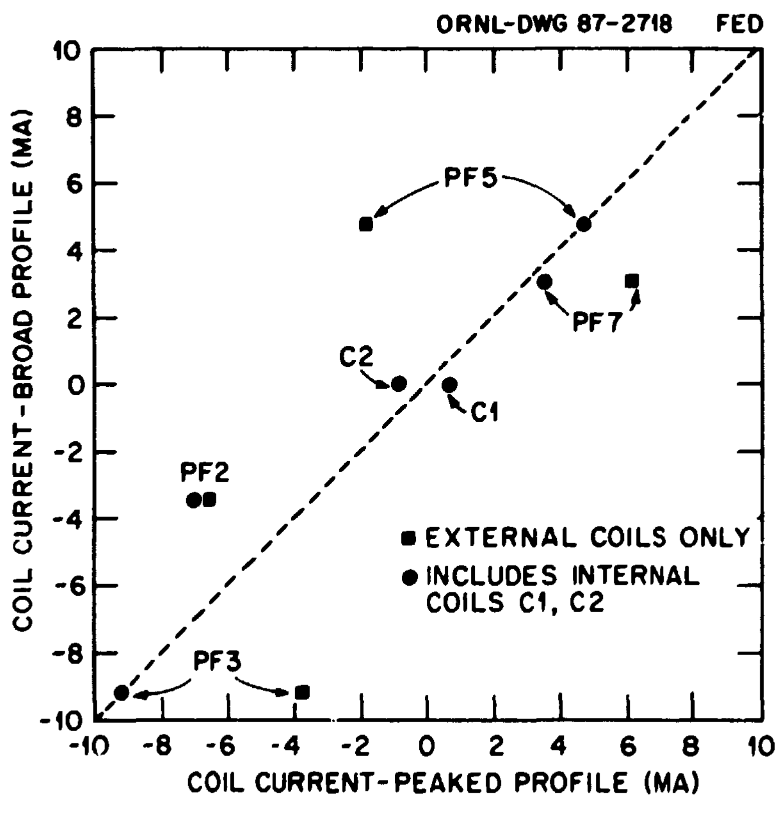

Fig. 7. Variation in poloidal field coil current with plasma current profile.

6. CONCLUSIONS

Forcing the separatrix flux surface to coincide with four prescribed points in the poloidal plane, over some range of uncertainty in plasma pressure and current profiles, requires four relatively independent coil groups. The degree of independence in these coil groups is often limited by physical constraints on their locations, which can result in large variations in coil currents due to profile uncertainty. This variation in the coil current distribution provides a measure for evaluating coil systems and changes in coil positions.

This study shows the feasibility of using external PF coils to position and shape the plasma flux surfaces relative to divertor plate strike points, but it points out inadequacies in relying entirely on an external coil set in the CIT.

ACKNOWLEDGMENTS

This work benefited greatly from discussions at Compact Ignition Tokamak Poloidal Field System workshops and with R. D. Pillsbury and R. J. Thome, in particular. The authors wish to thank Shirlene Dale for her careful preparation of the paper.

REFERENCES

1. R. Gallix, *CIT Divertor Plate Profile Study*, Memo B-861204-G-01, GA Technologies, Inc., San Diego, Calif., December 1986.

2. J. A. Schmidt et al., "A Compact Ignition Experiment," in *Proceedings of the 11th International Conference on Plasma Physics and Controlled Nuclear Fusion Research (Kyoto, 1986)*, International Atomic Energy Agency, Vienna, in press.

3. R. J. Thome, ed., *Poloidal Field Coil System Design for the Compact Ignition Tokamak (CIT)*, PFC/RR-86-11, Massachusetts Institute of Technology Plasma Fusion Center, Cambridge, Mass., April 1986.

4. D. J. Strickler, J. B. Miller, K. E. Rothe, and Y-K. M. Peng, *Equilibrium Modeling of the TFCX Poloidal Field Coil System*, ORNL/FEDC-83/10, Oak Ridge Natl. Lab., April 1984.

5. J. J. Moré, B. S. Garbow, K. E. Hillstrom, *User Guide for MINPACK-1*, ANL-80-74, Argonne Natl. Lab., Argonne, Ill., 1980.

6. F. Troyon, T. Gruber, H. Saurenmann, S. Semenzato, and S. Succi, *Plasma Phys. Controlled Fusion* **26**(1A), 209 (1984).

ORNL/FEDC-87/2
Dist. Category UC-20c,d

INTERNAL DISTRIBUTION

1.	T. G. Brown	19.	J. Sheffield
2.	L. A. Charlton	20–21.	Laboratory Records Department
3.	C. A. Flanagan	22.	Laboratory Records, ORNL-RC
4.	R. H. Fowler	23.	Central Research Library
5.	J. D. Galambos	24.	Document Reference Section
6.	J. A. Holmes	25.	Fusion Energy Division Library
7–11.	Y-K. M. Peng	26–27	Fusion Energy Division Publications Office
12.	R. L. Reid	28.	ORNL Patent Office
13.	T. E. Shannon		
14–18.	D. J. Strickler		

EXTERNAL DISTRIBUTION

29. M. A. Abdou, Boelter Hall, University of California, Los Angeles, CA 90024
30. C. A. Anderson, Westinghouse Electric Corporation, Advanced Energy Systems Division, P.O. Box 158, Madison, PA 15663
31. J. L. Anderson, CMB-3, Mail Stop 348, Los Alamos National Laboratory, P.O. Box 1633, Los Alamos, NM 87545
32. C. C. Baker, Argonne National Laboratory, 9700 South Cass Avenue, Argonne, IL 60439
33. D. S. Beard, Office of Fusion Energy, Office of Energy Research, ER-531 Germantown, U.S. Department of Energy, Washington, DC 20545
34. K. L. Black, Department E452, McDonnell Douglas Astronautics Company, P.O. Box 516, St. Louis, MO 63166
35. R. Botwin, C47-05, Grumman Aerospace Corporation, P.O. Box 31, Bethpage, NY 11714
36. W. B. Briggs, McDonnell Douglas Astronautics Company, P.O. Box 516, St. Louis, MO 63166
37. J. N. Brooks, FPP/207, Argonne National Laboratory, 9700 South Cass Avenue, Argonne, IL 60439
38. S. C. Burnett, GA Technologies, Inc., P.O. Box 81608, San Diego, CA 92138
39. J. D. Callen, Department of Nuclear Engineering, University of Wisconsin, Madison, WI 53706

40. R. N. Cherdack, Burns and Roe, Inc., 800 Kinderkamack Road, Oradell, NJ 07649
41. J. F. Clarke, Director for Fusion Energy, Office of Energy Research, ER-50 Germantown, U.S. Department of Energy, Washington, DC 20545
42. D. R. Cohn, 167 Albany Street, NW 16-140, Massachusetts Institute of Technology, Cambridge, MA 02139
43. R. W. Conn, Department of Chemical, Nuclear, and Thermal Engineering, Boelter Hall, University of California, Los Angeles, CA 90024
44. J. G. Crocker, EG&G Idaho, P.O. Box 1625, Idaho Falls, ID 83401
45. G. R. Dalton, Department of Nuclear Engineering Science, Nuclear Science Center, University of Florida, Gainesville, FL 32611
46. R. C. Davidson, Massachusetts Institute of Technology, 77 Massachusetts Avenue, Cambridge, MA 02139
47. N. A. Davies, Office of the Associate Director, Office of Fusion Energy, Office of Energy Research, ER-51 Germantown, U.S. Department of Energy, Washington, DC 20545
48. S. O. Dean, Director, Fusion Power Associates, Inc., 2 Professional Drive, Suite 249, Gaithersburg, MD 20760
49. D. DeFreece, E451, Building 81/1/B7, McDonnell Douglas Astronautics Company, P.O. Box 516, St. Louis, MO 63166
50. J. N. Doggett, L-441, Lawrence Livermore National Laboratory, P.O. Box 5511, Livermore, CA 94550
51. H. Dreicer, Division Leader, CRT, Los Alamos National Laboratory, P.O. Box 1663, Los Alamos, NM 87545
52. F. Farfaletti-Casali, Engineering Division, Joint Research Center, Ispra Establishment, 21020 Ispra (Varese), Italy
53. P. A. Finn, Fusion Power Program, Argonne National Laboratory, 9700 South Cass Avenue, Argonne, IL 60439
54. H. K. Forsen, Bechtel Group, Inc., Research & Engineering, P.O. Box 3965, San Francisco, CA 94119
55. J. S. Foster, Jr., Building R4-2004, TRW Defense and Space Systems, 1 Space Park, Redondo Beach, CA 90278
56. T. K. Fowler, Associate Director for Magnetic Fusion Energy, L-436, Lawrence Livermore National Laboratory, P.O. Box 5511, Livermore, CA 94550
57. J. W. French, Princeton Plasma Physics Laboratory, P.O. Box 451, Princeton, NJ 08544
58. H. P. Furth, Director, Princeton Plasma Physics Laboratory, P.O. Box 451, Princeton, NJ 08544
59. J. G. Gavin, Jr., President, A01-11, Grumman Aerospace Corporation, P.O. Box 31, Bethpage, NY 11714

60. G. Gibson, Westinghouse Electric Corporation, Waltz Mill Site, P.O. Box 158, Madison, PA 15663
61. J. R. Gilleland, Lawrence Livermore National Laboratory, P.O. Box 5511, Livermore, CA 94550
62. M. Y. Gohar, Argonne National Laboratory, 9700 South Cass Avenue, Argonne, IL 60439
63. R. W. Gould, Department of Applied Physics, California Institute of Technology, Pasadena, CA 91125
64. R. A. Gross, Plasma Research Laboratory, Columbia University, New York, NY 10027
65. J. R. Haines, McDonnell Douglas Astronautics Company, St. Louis, MO 63166
66. C. D. Henning, Lawrence Livermore National Laboratory, P.O. Box 5511, Livermore, CA 94550
67. J. J. Holmes, Westinghouse-Hanford Engineering Development Laboratory, P.O. Box 1970, Richland, WA 99352
68. T. Horie, Japan Atomic Energy Research Institute, Tokai Research Establishment, Tokai-Mura, Naka-Gun, Ibaraki-ken 319-11, Japan
69. J. B. Joyce, Princeton Plasma Physics Laboratory, P.O. Box 451, Princeton, NJ 08544
70. R. A. Krakowski, CTR-12, Mail Stop 641, Los Alamos National Laboratory, P.O. Box 1663, Los Alamos, NM 87545
71. G. L. Kulcinski, University of Wisconsin, Department of Nuclear Engineering, Engineering Research Building, Room 439, 1500 Johnson Drive, Madison, WI 53706
72. D. L. Kummer, McDonnell Douglas Astronautics Company, P.O. Box 516, St. Louis, MO 63166
73. W. Marton, Office of Fusion Energy, Office of Energy Research, ER-55 Germantown, U.S. Department of Energy, Washington, DC 20545
74. L. G. Masson, EG&G Idaho, Idaho National Engineering Laboratory, P.O. Box 1625, Idaho Falls, ID 83401
75. D. M. Meade, Princeton Plasma Physics Laboratory, P.O. Box 451, Princeton, NJ 08544
76. A. T. Mense, Building 107, Post B2, McDonnell Douglas Astronautics Company, P.O. Box 516, St. Louis, MO 63166
77. R. W. Moir, Lawrence Livermore Laboratory, P.O. Box 5511, Livermore, CA 94550
78. D. B. Montgomery, MIT Plasma Fusion Center, 167 Albany Street, Cambridge, MA 02139
79. A. E. Munier, Grumman Aerospace Corporation, P.O. Box 31, Bethpage, NY 11714
80. R. E. Nygren, FPP/207, Argonne National Laboratory, 9700 South Cass Avenue, Argonne, IL 60439

81. T. Ohkawa, GA Technologies, Inc., P.O. Box 81608, San Diego, CA 92138
82. J. A. O'Toole, Princeton Plasma Physics Laboratory, James Forrestal Campus, Building I-P, Room 8A, P.O. Box 451, Princeton, NJ 08544
83. R. R. Parker, Francis Bitter National Magnet Laboratory, 170 Albany Street, Cambridge, MA 02139
84. B. Pease, Culham Laboratory, Abingdon, Oxfordshire OX14 3DB, United Kingdom
85. M. Pelovitz, Princeton Plasma Physics Laboratory, P.O. Box 451, Princeton, NJ 08544
86. F. W. Perkins, Princeton Plasma Physics Laboratory, P.O. Box 451, Princeton, NJ 08544
87. M. Porkolab, Massachusetts Institute of Technology, 77 Massachusetts Avenue, Cambridge, MA 02139
88. D. E. Post, Princeton Plasma Physics Laboratory, P.O. Box 451, Princeton, NJ 08544
89. R. E. Price, Office of Fusion Energy, Office of Energy Research, ER-55 Germantown, U.S. Department of Energy, Washington, DC 20545
90. F. A. Puhn, GA Technologies, Inc., P.O. Box 81608, San Diego, CA 92138
91. R. V. Pyle, University of California, Lawrence Berkeley Laboratory, Berkeley, CA 94720
92. J. M. Rawls, GA Technologies, Inc., P.O. Box 81608, San Diego, CA 92138
93. M. Roberts, International Program, Office of Fusion Energy, Office of Energy Research, ER-52 Germantown, U.S. Department of Energy, Washington, DC 20545
94. J. D. Rogers, Los Alamos National Laboratory, P.O. Box 1663, Los Alamos, NM 87545
95. M. L. Rogers, Monsanto Research Corporation, Mound Laboratory Facility, P.O. Box 32, Miamisburg, OH 45342
96. M. N. Rosenbluth, RLM 11.218, Institute for Fusion Studies, University of Texas, Austin, TX 78712
97. P. H. Rutherford, Princeton Plasma Physics Laboratory, P.O. Box 451, Princeton, NJ 08544
98. J. A. Schmidt, Princeton Plasma Physics Laboratory, P.O. Box 451, Princeton, NJ 08544
99. J. Schultz, MIT Plasma Fusion Center, 167 Albany Street, Cambridge, MA 02139
100. F. R. Scott, Electric Power Research Institute, P.O. Box 10412, Palo Alto, CA 94304
101. G. Sheffield, Princeton Plasma Physics Laboratory, P.O. Box 451, Princeton, NJ 08544

102. D. Smith, Materials Science Division, Argonne National Laboratory, 9700 South Cass Avenue, Argonne, IL 60439
103. W. M. Stacey, Jr., Georgia Institute of Technology, School of Nuclear Engineering and Health Physics, Atlanta, GA 30332
104. D. Steiner, Rensselaer Polytechnic Institute, Nuclear Engineering Department, NES Building, Tibbets Avenue, Troy, NY 12181
105. E. Stern, Grumman Aerospace Corporation, CN-59, Forrestal Campus, Princeton, NJ 08544
106. P. M. Stone, Fusion Systems Design Branch, Division of Development and Technology, Office of Fusion Energy, Office of Energy Research, ER-532 Germantown, U.S. Department of Energy, Washington, DC 20545
107. I. N. Sviatoslavsky, Room 33, Engineering Research Building, 1500 Johnson Drive, University of Wisconsin, Madison, WI 53706
108. R. E. Tatro, Manager, Energy Systems, M.Z. 16-1070, General Dynamics-Convair Division, P.O. Box 80847, San Diego, CA 92138
109. F. Thomas, B-20-5, Grumman Aerospace Corporation, Bethpage, NY 11714
110. K. I. Thomassen, Lawrence Livermore National Laboratory, P.O. Box 5511, Livermore, CA 94550
111. R. J. Thome, Francis Bitter National Magnet Laboratory, 170 Albany Street, Cambridge, MA 02139
112. C. Trachsel, McDonnell Douglas Astronautics Company, P.O. Box 516, St. Louis, MO 63166
113. A. W. Trivelpiece, Office of Energy Research, U.S. Department of Energy, Washington, DC 20545
114. L. R. Turner, Fusion Power Program, Argonne National Laboratory, 9700 South Cass Avenue, Argonne, IL 60439
115. E. H. Valeo, Princeton Plasma Physics Laboratory, P.O. Box 451, Princeton, NJ 08544
116. R. Varma, Physical Research Laboratory, Navrangpura, Ahmedabad 380009, India
117. J. C. Wesley, GA Technologies, Inc., P.O. Box 81608, San Diego, CA 92138
118. J. E. C. Williams, Francis Bitter National Magnet Laboratory, 170 Albany Street, Cambridge, MA 02139
119. H. H. Yoshikawa, W/A-62, Hanford Engineering Development Laboratory, P.O. Box 1970, Richland, WA 99352
120. K. M. Young, Princeton Plasma Physics Laboratory, P.O. Box 451, Princeton, NJ 08544
121. N. E. Young, Princeton Plasma Physics Laboratory, P.O. Box 451, Princeton, NJ 08544

122. Bibliothek, Max-Planck Institut fur Plasmaphysik, D-8046 Garching, Federal Republic of Germany
123. Bibliothek, Institut fur Plasmaphysik, KFA, Postfach 1913, D-5170 Julich, Federal Republic of Germany
124. F. Prevot, CEN/Cadarache, Departement de Recherches sur la Fusion Controlee, 13108 Saint-Paul-lez-Durance, France
125. Bibliotheque, CEN/Cadarache, 13108 Saint-Paul-lez-Durance, France
126. Library, Centre de Recherches en Physique des Plasmas, 21 Avenue des Bains, 1007 Lausanne, Switzerland
127. Library, Culham Laboratory, UKAEA, Abingdon, Oxfordshire, OX14 3DB, England
128. Library, FOM Instituut voor Plasmafysica, Rijnhuizen, Edisonbaan 14, NL-3430 Nieuwegein, The Netherlands
129. J. Shang-Xian, Graduate School, Academia Sinica, P.O. Box 3908, Beijing, China (PRC)
130. Library, Institute for Plasma Physics, Nagoya University, Nagoya 464, Japan
131. Library, International Centre for Theoretical Physics, Trieste, Italy
132. Library, JET Joint Undertaking, Abingdon, Oxfordshire, OX14 3EA, England
133. Library, Laboratorio Gas Ionizzati, CP 65, 00044 Frascati, Rome, Italy
134. Plasma Research Laboratory, Australian National Laboratory, P.O. Box 4, Canberra, ACT 2000, Australia
135. Thermonuclear Library, Japan Atomic Energy Research Institute, Tokai Research Establishment, Tokai-Mura, Naka-Gun, Ibaraki-ken 319-11, Japan
136. Library, Plasma Physics Laboratory, Kyoto University, Gokasho, Uji, Kyoto 611, Japan
137. Office of the Assistant Manager for Energy Research and Development, U.S. Department of Energy, Oak Ridge Operations, P.O. Box E, Oak Ridge, TN 37831

138–277. Given distribution as shown in TIC-4500, Magnetic Fusion Energy (Distribution Category UC-20 c,d: Reactor Materials and Fusion Systems)